REGIONAL MAPPING OF PLANT FUNCTIONAL TYPES IN RIVER FLOODPLAIN ECOSYSTEMS USING AIRBORNE IMAGING SPECTROSCOPY DATA

L. Kooistra *, L. Sanchez-Prieto , H.M. Bartholomeus, M.E. Schaepman

Wageningen University, Centre for Geo-Information, Droevendaalsesteeg 3, NL-6708 PB Wageningen, The Netherlands

Commission VII, WG VII/1

KEY WORDS: imaging spectroscopy, spectral mixture analysis, plant functional types, plant traits, dynamic vegetation model

ABSTRACT:

Monitoring and forecasting of natural vegetation succession is essential for optimal management of river floodplain ecosystems in Western Europe. For example the development of woody vegetation types (e.g., softwood forest) increases the hydraulic resistance of the floodplain and can have negative effects on the discharge capacity of the river. However, from a biodiversity point-of-view this development results in higher valued nature reserves. The current challenge for river managers is therefore how to combine sustainable flood protection and floodplain rehabilitation in the best possible way. Natural vegetation in these floodplain ecosystems consists of a continuum between grassland and forest. Ground coverage by woody plants (trees and shrubs) ranges from non-existent to complete and forms a mosaic pattern within the ecosystem.

Dynamic vegetation modeling becomes an increasingly important tool to assess the current and future state of these complex ecosystems. In this approach, remote sensing is used to derive spatial continuous input date of the state of the ecosystem to initialize these models at simulation start. Also site-specific remote sensing derived variables (e.g., LAI, biomass, canopy N) are assimilated in these models resulting in more reliable and accurate predictions. Interfacing between remote sensing and dynamic vegetation models requires a proper representation of the grassland-forest continuum. For global scale modeling, plant functional types (PFT), i.e., groups of plant species that share similar functioning are adopted to represent vegetation distribution and derived using remote sensing based methods. Also on a regional scale the use of PFTs could be of interest to map vegetation heterogeneity through separately specifying the composition and structure of PFTs within a grid cell.

In this study we investigate the possibilities to derive the spatial distribution of PFTs for floodplain ecosystems from imaging spectroscopy data at the regional level. Field and airborne data (HyMap) were acquired for a floodplain along the river Rhine in the Netherlands and used to derive spatial continuous PFT maps. Spectra of main PFTs (grass, herbs, shrub, and trees) were selected from the image data and identified as endmembers using a site-specific library. The results show that spectral unmixing analysis can be used for mapping plant functional types to characterize the complex structure and composition of a natural floodplain ecosystem. Spatial distributions of herbaceous and tree PFTs are well in agreement with actual situation as observed in the field. Modelled fractional coverage of the herbaceous PFTs agreed reasonable well with field observed abundances (R^2 between 0.35 and 0.56). Further work is required to upscale the approach from the floodplain level to the river catchment scale using medium-resolution sensors like MODIS and MERIS.

1. INTRODUCTION

Monitoring and forecasting of natural vegetation succession is essential for optimal management of river floodplain ecosystems in Western Europe. For example the development of woody vegetation types (e.g., softwood forest) increases the hydraulic resistance of the floodplain and can have negative effects on the discharge capacity of the river. Natural vegetation in these floodplain ecosystems consists of a continuum between grassland and forest. Ground coverage by woody plants (trees and shrubs) ranges from non-existent to complete and forms a mosaic pattern within the ecosystem (Ward *et al.*, 2002).

Increasingly, dynamic vegetation models (DVM) are being used to model the influence of natural vegetation succession on river discharge and flooding patterns (Baptist *et al.*, 2004). Traditional characterisation of vegetation dynamics by using aerial photograph derived vegetation or ecotope maps do not fulfil modelling requirements. The derived vegetation polygons consist of mixed units with a complex structure which cannot directly be linked to hydrodynamic processes.

For global scale climate modelling, plant functional types (PFT), i.e., groups of plant species that share similar functioning are adopted to represent vegetation distribution and derived using remote sensing based methods (Bonan *et al.*, 2003). Also on a regional level, several dynamic vegetation models use a PFT based approach which defines it as a group of species that share traits (morphological and physiological attributes) and play a similar role in a ecosystem (Paruelo and Lauenroth, 1996). Plant traits which influence water flow in floodplain systems (e.g., height, flexibility, density) have been identified in earlier studies (Anderson *et al.*, 2006) and could be used as a basis for the definition of PFTs.

Also on a regional scale, remote sensing based techniques would be the most appropriate method to survey the heterogeneous vegetation composition of a natural floodplain. This paper explores the possibilities to derive the spatial distribution of PFTs for floodplain ecosystems from imaging spectroscopy data. We are especially interested in the opportunities of imaging spectroscopy data to separately specify the composition and structure of PFTs within a grid

* Corresponding author: e-mail Lammert.Kooistra@wur.nl

cell. Spectral mixture analysis (SMA) (Smith *et al.*, 1985) is examined as a possible tool that takes advantage of the high-dimensional spectral information content of imaging spectroscopy data to discriminate PFTs at the sub-pixel level, thus overcoming possible limitations in spatial resolution.

2. MATERIAL AND METHODS

2.1 Study area

The Millingerwaard floodplain (51º84'N, 5º99' E) along the river Waal in the Netherlands was chosen for this study. The floodplain is part of the Gelderse Poort nature reserve and considered a nature rehabilitation area, meaning that for some time now areas have been taken out of agricultural production and are allowed to undergo natural succession. This has resulted in a heterogeneous landscape (Figure 1) with river dunes covered by pioneer vegetation (MNV) along the river, a large softwood forest in the eastern part along the winterdike (MWT) and in the intermediate area a mosaic pattern of different succession stages ranging from herbaceous (RNV) to shrubs (SWS, MWS) and areas influenced by grazing (SNV). Nature management (e.g., grazing) within the floodplain is aiming at improvement of biodiversity. In addition, measures for reduction of the hydraulic resistance of the vegetation (e.g., harvesting of softwood forest) have been carried out. Plant functional types were defined as vegetation clusters with similar impact to water flow impact and were identified based on three plant traits (Anderson *et al.*, 2006): height, flexibility and density (Table 1).

Plant Functional Type	**Height** (m)	**Flexibility**[1] (cm)	**Density**[2]
Soft Non-woody Vegetation (SNV)	0 - 0.5	<1	Herbaceous
Medium Non-woody Vegetation (MNV)	0.5 - 1	<1	Herbaceous
Robust Non-woody Vegetation (RNV)	1 - 2	<1	Herbaceous
Soft Woody vegetation with Shrub structure (SWS)	0.5 - 4	0 - 5	Shrub
Medium Woody vegetation with Shrub structure (MWS)	0.5 - 10	5 - 15	Shrub
Medium Woody Vegetation with Tree structure (MWT)	0.5 - 35	5 - 15	Tree

1: based on stem thickness; 2: based on species composition

Table 1. Main plant functional types for vegetation in floodplain Millingerwaard along the river Waal in the Netherlands

2.2 Data

Imaging spectrometer data for the Millingerwaard were acquired on July 28, 2004 using the HyMap sensor in 126 spectral bands ranging from 400 to 2500 nm (bandwidth 15 - 20 nm). The data were processed to surface reflectance by partially compensating for adjacency effects and directional effects using the model combination PARGE/ATCOR-4 (Richter and Schläpfer, 2002). The spatial resolution of the images is 5 m. Ground measurements include top-of-canopy reflectance measurements as well as leaf optical properties measurements at all ground plots as well as several reflectance measurements of calibration surfaces using an ASD FieldSpec instrument. A mask was applied to select the Millingerwaard floodplain and to remove all areas covered with water (river and lakes).

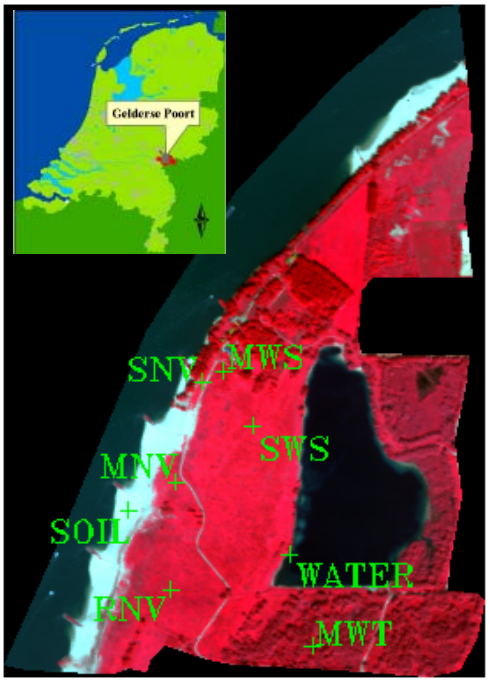

Figure 1. HyMap image for the Millingerwaard floodplain along the river Waal. The indicated points show the location of 'pure' PFTs from the field polygons for which spectral endmembers were derived from the image. Inset shows the location of the floodplain within the Gelderse Poort nature reserve.

Three field datasets describing species composition and vegetation structure were available for the floodplain. In 2004 and 2005, vegetation relevees were made according to the method of Braun-Blanquet in 2x2 m plots for 21 and 14 locations, respectively. Abundance per species was estimated optically as percentage soil covered by living biomass in vertical projection, and scored in a nine-point scale. The coordinates of the central location of each ground plot was determined using a differential global positioning system. Part of the 2004 and 2005 datasets were used for endmember selection while the rest of locations was used to assess the accuracy of the spatial distributions for the PFTs SNV, MNV and RNV. A third dataset consisted of a database provided by the Ark Nature Foundation with GPS measured field locations of all individual shrub and tree species in the central part of the floodplain. For every shrub and tree, parameters like stem diameter, height, volume and species type were recorded. This database was used to assess the accuracy of the spatial distribution for the PFTs SWS and MWS which both consist of vegetation with a shrub structure.

2.3 Endmember selection and spectral unmixing

As the vegetation structure within the floodplain is highly heterogeneous, we expect that the measured spectral signal for every pixel is the result of fractions in which different PFTs and also the soil background occur. Since we are interested in these fractions, spectral mixture analysis (SMA) was applied. This method assumes that a value at a given pixel is the result of a linear combination of one or more components, or endmembers (Tompkins *et al.*, 1997). The application of SMA to an image to identify PFTs requires a careful selection of endmembers related to two aspects: a) an actual list of endmembers to

include and b) identification of potential endmembers (Rosso *et al.*, 2005). For image-based extraction of endmembers, several algorithms are available (Plaza *et al.*, 2004) and have been applied in earlier vegetation studies: e.g., PPI (Schmid *et al.*, 2005; Rosso *et al.*, 2005) or SSA (Bateson *et al.*, 2000).

In our study, we used a manual approach based on field data for endmember selection. Based on the available field information, candidate pixels were selected from locations were the PFTs appeared pure or had a relative homogeneous species composition. Candidate pixels for endmember extraction of the PFTs SNV, MNV and RNV were selected using the vegetation relevees acquired in 2004 and 2005. Selection of endmember spectra for the PFTs SWS, MWS and MWT was based on the Ark database. The database was used to derive point density grid of the number of individual shrub and trees species within a 5 m pixel according to the HyMap pixel size. Pixels with the highest number of shrub and tree locations were used to derive endmember spectra for the PFTs SWS, MWS and MWT. Final locations for the selected endmembers are presented in Figure 1.

A forward minimum noise fraction (MNF) (Green *et al.*, 1988) transformation was applied to the HyMap image to reduce interband correlation and data redundancy. The MNF analysis showed that the first eigenimage had an eigenvalue of 105.1; by the 10th eigenimage the eigenvalue dropped to 6.8, and after the 30th, eigenvalues became asymptotic between around 1.3. By the 25th eigenimage most of the structural features of the floodplain disappeared, indicating increasing noise content. As a result, the first 30 bands with an eigenvalue were used for SMA. The SMA algorithm implemented in ENVI was used for this study. This algorithm provides no fully constrained option. However, for the constraint that fractions should sum up to one, a weight of 1000 was assigned.

2.4 Accuracy assessment

To assess the accuracy of SMA for mapping the abundance of PFTS in the Millingerwaard, three methods were used. First, the fit of the SMA model was assessed based on the spatial continuous map for the root mean square error (RMSE). Higher values of RMSE indicate regions that could contain lacking endmembers. Secondly, the dataset with actual PFTs abundances from the field in 2004 and 2005 was compared to SMA modelled abundances for these observations. As a third method, the locations of the two main shrub species available in the database of the Ark Foundation was overlaid with the abundance maps of SWS and MWS.

3. RESULTS AND DISCUSSION

3.1 Endmember selection

Six endmembers indicating different PFTs (Table 1) and a soil endmember were used as input to SMA for the Millingerwaard (Figure 2). Main differences between the PFT endmembers can be observed in the reflectance around the green (550 nm) and red (650 nm) band, around the liquid water absorption features at 970 nm and 1200 nm and large difference in intensity over the NIR and SWIR wavelength region. The soil endmember exhibits high reflectance across the entire spectral range. Small absorption features around 2250 nm and 2350 nm indicate low clay and carbonate mineral concentrations in the soil.

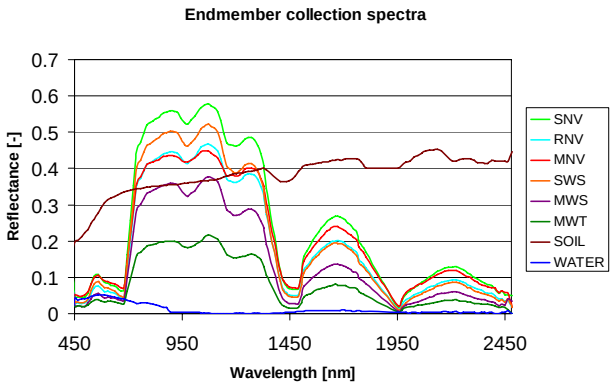

Figure 2. Spectral plot of seven endmembers used with SMA

3.2 Fraction images

SMA generated seven fraction images (six PFTs and soil) and a RMSE image. The spatial distribution of the PFTs in the fraction images (Figure 3) show clear patterns which agree with the observed situation in the field. The coverage of SNV is characterized by dense short (grazed) grassland vegetation and occurs in several areas of the floodplain (Figure 3). A clear hotspot can be observed in a triangular area in the north of the floodplain which is a former agricultural field under grazing management. In the central area of the floodplain, smaller grazing areas and paths which are used by cattle can be identified. Abundance of MNV is mainly located on the sandy levee along the river. This PFT is characterized by a relatively open structure and influence of the soil background in the reflectance signal (Figure 4). Apart from the levee, the PFT MNV is also abundant in the Northern part of the floodplain where the upper clay layer has been removed until the sandy subsoil. The resulting vegetation is dominated by pioneer species and has a relatively open structure.

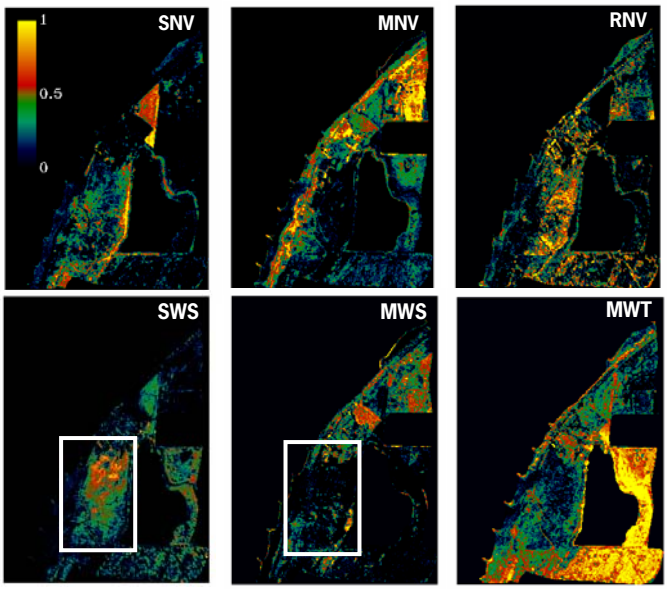

Figure 3. Fraction images per plant functional type in the Millingerwaard. The rectangles for SWS and MWS show the areas which were compared with the database of the Ark Foundation (Figure 6).

The coverage of RNV, which is dominated by *Rubus caesius* and *Urtica dioica*, is mainly concentrated in the central area of the floodplain. This area was formerly used as arable land with a relatively high nutrient input. This has resulted in natural vegetation with a dense structure and a high productivity. In addition, this PFT is also found as main understory of the softwood forest (MWT), indicated by the patchy abundance in the south-eastern part of the floodplain where the softwood forest is located. The process of shrub encroachment can be clearly observed from the spatial distribution of SWS (Figure 3) which is dominated by *Crataegus monogyna*. The direction of this process is from the North-eastern part within the indicated rectangle to the South-west. The vegetation of MWS is characterized by the presence of *Samubucus Nigra* and the fraction map shows that this PFT is abundant in some concentrated areas of the floodplain.

Comparison of the spatial pattern of MWS with the actual situation shows that not only vegetation with a shrub structure is classified as having a high abundance but also a part of the tree dominated areas. Some areas with increased coverage of the tree species *Populus* are confused with the shrub based PFT MWS. This confusion between MWS and MWT could be explained by the overlap in these two classes where main differences are related to height and species composition. Forested areas dominated by willow trees (*Salix fragilis* and *Salix Alba*) are mainly classified as MWT. The high abundance of MWT in the South-eastern part of the floodplain is explained by the relatively lower and wet position of this area resulting in a high abundance of willow trees. Areas with a MWT abundance below 0.5 depicted as green in the fraction image (Figure 3) do not agree with the actual situation. These areas are mainly covered by vegetation with a herbaceous structure (SNV, MNV). Possibly, the SMA algorithm uses the MWT endmember to compensate for the lower spectral reflectance in these areas due to lower vegetation coverage. Going from the sandy beaches along the river a small transitional area with decreasing abundance of soil can be observed (Figure 4). However, in the central part of the floodplain the abundance of open soil as modelled by SMA is relatively low.

3.3 Accuracy assessment

The RMSE map was used for a first assessment of the accuracy of the PFT fraction images generated for the Millingerwaard. Higher values of RMSE indicate regions that could contain lacking endmembers. High RMSE values for the forested area in the centre of the image can be explained by the choice of the MWT endmember (Figure 1). The vegetation structure of the

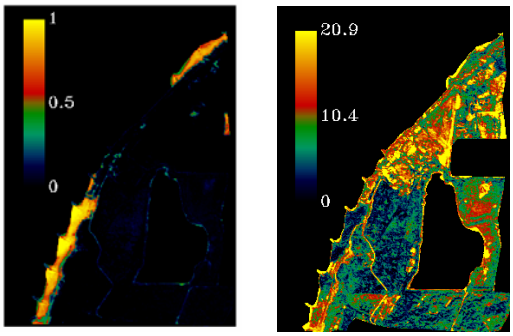

Figure 4. Fraction image for soil endmember (right) and RMSE image (left) in the Millingerwaard.

latter endmember was characterized by a dense coverage of willow trees, while for the central forest area the structure has a more open character while also species coverage is more divers (including *Populus*). High RMSE values in the willow forest in the Eastern part of the floodplain can be explained by presence of small lakes which are covered by willow trees. As a result mixed pixels are present with both influence of water and vegetation. However, an endmember for water was not included in our analysis, resulting in increased values for RMSE. High RMSE values along the river are explained by the heterogeneous coverage of the groins (e.g., vegetation, stones of basalt rock) and the influence of wet soils along the shores of the river. Finally, in our endmember set we have not accounted for a shadow component (Li *et al.*, 2005). This could be especially relevant for forest edges, hedges with a composition of both shrub and trees and for locations with individual large trees. Removal of the errors related to non-vegetated areas (e.g., rock, soil, water, dust road etc.) could be achieved by using an effective VI-based masking procedure (e.g., NDVI). However, as vegetation coverage is abundant related to the spatial resolution of the HyMap image (5 m) complete removal of all non-vegetated components is difficult.

Comparison of the predicted vs. observed coverage for the herbaceous PFTs SNV, MNV and RNV shows a reasonable agreement as indicated by R^2 values of 0.56, 0.35 and 0.43, respectively. Negative fractions for some of the plots are explained by the fact that for this study we used an unconstrained implementation of the SMA algorithm. However, no large negative values were derived using SMA. In general fractions for all three herbaceous PFTs are underestimated. Comparison of the individual plots with the expected one-to-one line shows that this is especially the case for SNV and to a lesser extent for MNV and RNV. This can

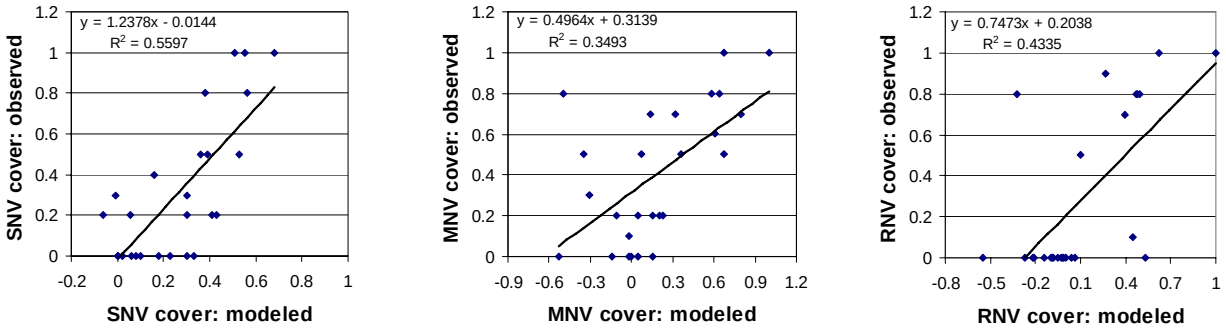

Figure 5. Comparison of results from predicted fractions using SMA and fractions observed in field plots in 2004 and 2005 (n = 26) for PFTs SNV, MNV and RNV, respectively.

partly be explained by the difference in the sample units of the vegetation relevee (2x2 m) and the spatial resolution of the HyMap image (5x5 m). For this study we assumed that the PFT abundances in the plot of the vegetation relevee are representative for the co-located HyMap pixel. However, especially the spatial structure for SNV is relatively narrow (e.g., grazing paths) with small areas with a homogeneous coverage. This means that translation of the field relevee abundances to the HyMap pixel resolution, results in an overestimation of the SNV abundance for the field observed value in Figure 5.

Plots which are located on the x-axis in Figure 5 indicate that the SMA model calculates the presence of a certain PFT while in the field situation this PFT is not abundant. Overestimation for these fractions shows maximum values up to 0.3, 0.2 and 0.48 for SNV, MNV and RNV respectively.

The accuracy of the estimated fractions for the PFTs SWS and MWS was assessed through a comparison of the fraction images with the locations of individual shrub stands (database Ark Foundation) for the central part of the Millingerwaard (Figure 6). Differences between SWS and MWS are related to height of the vegetation and the thickness of the stem (or 'flexibility') as indicated in Table 1. Based on this difference we related the location of the *Crataegus monogyna* (n=2100) to the SWS fraction image and the location of *Samubucus Nigra* (n=1254) to the MWS fraction image. The comparison shows (Figure 6) that there is a reasonable agreement between individual shrub locations and areas with a relatively high abundance of SWS and MWS. However, high abundance of SWS is not only related to *Crataegus monogyna* but also to *Samubucus Nigra*, while certain patterns for MWS are also related to the presence of *Crataegus monogyna*. This agrees with the concept of PFTs where differences between vegetation units are related to their plant traits instead of their species composition. In addition, the comparison shows that younger shrub plants which are mainly located in the southern part of the floodplain are not always recognized. This could be explained by their spectral resemblance to the rough herbaceous PFTs. In this analysis we did not include available information on species height and volume which could be used to get a better explanation of the spatial structures in the fraction images of SWS and MWS.

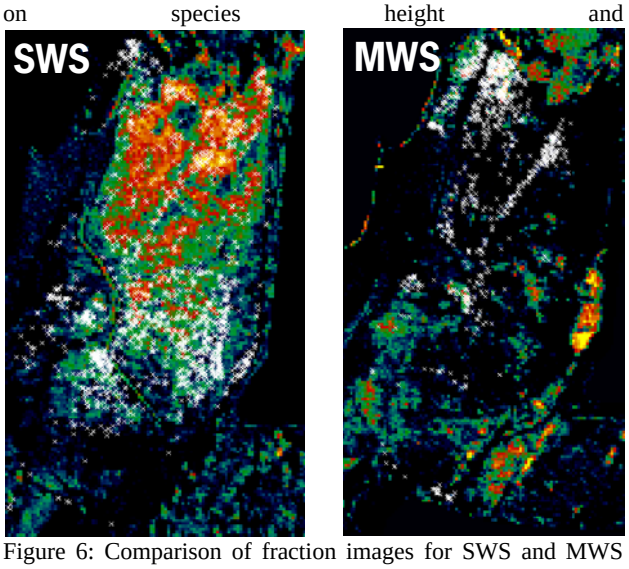

Figure 6: Comparison of fraction images for SWS and MWS with the locations for individual species of *Crataegus monogyna* (n=2100) and *Samubucus Nigra* (n=1254), respectively. Locations were taken from the database of the Ark Foundation

Experience of nature managers within the floodplain Millingerwaard indicates that vegetation succession in the floodplain has resulted in a gradual increase of shrub coverage at the expense of grass and herbaceous vegetation types. In this study we focussed on mapping of PFTs. However, based on available hyperspectral data for 2001 and 2005 for this floodplain, we will investigate the possibilities of these data in combination with SMA to monitor these shrub encroachment processes.
In a next step, these imaging spectroscopy derived vegetation variables (e.g., PFT, LAI, biomass, vegetation structure) can be used for initialization and calibration of dynamic vegetation models with the objective to test ecological hypotheses or to assess and forecast the state of future landscapes (Kooistra *et al.*, 2007). In addition, further work is required to upscale the approach from the floodplain level to the river catchment scale using medium-resolution sensors like MODIS and MERIS.

4. CONCLUSIONS

This paper shows that SMA can be used for mapping plant functional types to characterize the complex structure and composition of a natural floodplain ecosystem. The results show that spatial distributions of herbaceous and tree PFTs are well in agreement with actual situation as observed in the field. For older plants, the spatial distribution of shrub PFTs is well in agreement with the field situation. Younger shrub plants are not always recognized which could be explained by their spectral resemblance to the rough herbaceous PFTs. The modelled fractional coverage of the herbaceous PFTs agreed reasonable well with field observed abundances with R^2 values ranging between 0.35 and 0.56. In this study we used a manual approach for endmember selection. Although the use of image based endmember extraction techniques would be of interest to investigate, our experience is that the use of field information is an important requirement for proper selection in complex vegetated areas.

ACKNOWLEDGMENTS

The authors wish to acknowledge the Belgian Science Policy Office for providing the HyMap data-set and Staatsbosbeheer for their permission to access the Millingerwaard test area. We would like to thank Bart Beekers and Johan Bekhuis of the Ark Nature Foundation for provision of the woody species database.

REFERENCES

Anderson, B.G., Rutherfurd, I.D., and Western, A.W., 2006. An analysis of the influence of riparian vegetation on the propagation of flood waves. *Environmental Modelling and Software*, 21, pp. 1290-1296.

Baptist, J.P., Ellis Penning, W., Duel, H., Smits, A.J.M., Geerling, G.W., Van der Lee, G.E.M., and Van Alphen, J.S.L., 2004. Assessment of the effects of cyclic rejuvenation on flood levels and biodiversity along the Rhine river. *River Research and Applications*, 20, pp. 285-297.

Bonan, G.B., Levis S., Sitch S., Vertenstein, M., Olenson K.W., 2003. A dynamic global vegetation model for use with climate

models; concepts and description of simulated vegetation dynamics. *Global Change Biology*, 9, pp. 1543-1566.

Green, A.A., Berman, M., Switzer, P., Craig, M.D., 1988. A transformation for ordering multispectral data in terms of image quality with implications for noise removal. *IEEE Trans. Geosci. Remote Sens.*, 26, pp. 65-74.

Kooistra, L., Wamelink, G.W.W., Schaepman-Strub, G., Schaepman, M., van Dobben, H., Aduaka, U., and Batelaan, O., 2007. Assessing and predicting biodiversity in a floodplain ecosystem: assimilation of Net Primary Production derived from imaging spectrometer data into a dynamic vegetation model. *Remote Sensing of Environment*, (submitted).

Li, L., Ustin, S.L., and Lay, M., 2005. Application of multiple endmember spectral mixture analysis (MESMA) to AVIRIS for coastal salt marsh mapping: a case study in China Camp, CA, USA. *International Journal of Remote Sensing*, 26, pp. 5193-5207.

Paruelo, J.M., Lauenroth, W.K., 1996. Relative abundance of plant functional types in grasslands and shrublands of North America. *Ecological Applications*, 6(4), pp. 1212-1224.

Plaza, A., Martinez, P., Perz, R., and Plaza, J., 2004. A quantitative and comparative analysis of endmember extraction algorithms from hyperspectral data. *IEEE Transactions on Geoscience and Remote Sensing*, 42, pp. 650-663.

Richter, R., and Schläpfer, D., 2002. Geo-atmospheric processing of wide FOV airborne imaging spectrometry data. In Proceedings of SPIE - The International Society for Optical Engineering, Vol. 4545, pp. 264.

Rosso, P.H., Ustin, S.L., and Hastings, A., 2005. Mapping marshland vegetation of San Francisco Bay, California, using hyperspectral data. *International Journal of Remote Sensing*, 26, pp. 5169-5191.

Schmid, T., Koch, M., and Gumuzzio, J., 2005. Multisensor approach to determine changes in wetland characteristics in semiarid environments (Central Spain). *IEEE Transactions on Geoscience and Remote Sensing*, 43, pp. 2516-2525.

Smith, M.O., Johnstonn, P.E., and Adams, J.B., 1985. Quantitative determination of mineral types and abundances from reflectance spectra using principal component analysis. *J. Geophys. Res.*, 90, pp. 797-804.

Tompkins, S, Mustard, J.F., Pieters, C.M., and Forsyth, D.W., 1997. Optimization of endmembers for spectral mixture analysis. Remote Sensing of Environment, 59, pp. 472-489.

Ward, J.V., Tockner, K., Arscott, D.B., and Claret, C., 2002. Riverine landscape diversity. *Freshwater Biology*, 47, pp. 517-539.